Radio Interferometry: Theory, Techniques and Applications,
IAU Coll. 131, ASP Conference Series, Vol. 19, 1991,
T.J. Cornwell and R.A. Perley (eds.)

249

THE FIRST VLA OBSERVATIONS OF RADIO SOURCES AT 73.8 MHz

N. E. KASSIM
Center for Advanced Space Sensing
Naval Research Laboratory
Washington, DC 20375-5000

R. A. PERLEY
National Radio Astronomy Observatory
Socorro, New Mexico 87801

W. C. ERICKSON
U. of Maryland
College, Park, Maryland 20744

ABSTRACT   73.8 MHz instrumentation for the VLA is being
developed and is currently installed on 8 VLA dishes.
Test observations of strong radio sources have been
made. We describe techniques that we have developed to
analyze these test observations and we present examples
of our first maps.

INTRODUCTION

We have begun testing a 73.8 MHz observing system at the VLA.
Currently 8 of the VLA's 25 meter dishes are outfitted with
73.8 MHz cross-dipole feeds situated at prime focus. The
aperture efficiency of the elements is about 25%, or about 125
m^2 per dish. When the whole array is instrumented at 73.8 MHz
it will have a total collecting area of approximately 3,400 m^2
and a sensitivity in the 10 mJy range. With angular
resolution of 20", this system would represent a major
improvement over any other low frequency system currently
available. Here we describe briefly some of the techniques we
have developed to analyze our test observations, and present
some high resolution maps of strong sources.

RFI REJECTION

Radio Frequency Interference (RFI) is a major problem at low
frequencies. We employ a 1.5 MHz band centered in the 73.0 to

74.6 MHz Radio Astronomy allocation. We find no external RFI
within this band, but strong signals at adjacent frequencies
cause considerable difficulty. These are the TV Channel 3
sound carrier at 71.75 MHz and strong RFI generated by the VLA
system at 75.0 MHz. There also exist signals from the "B"
racks of each VLA dish. These signals appear as narrow band
interference spikes in the cross-power spectrum as shown in
Fig. 1a (below). They are greatly reduced by shielding the
"B" rack as shown by the cross-power spectrum in Fig. 1b, and
their effects are eliminated by operating in the spectral line
mode and discarding the affected spectral channels. This
technique will not be effective as the array moves into more
compact configurations (i.e. "C" and "D" arrays), so more RFI
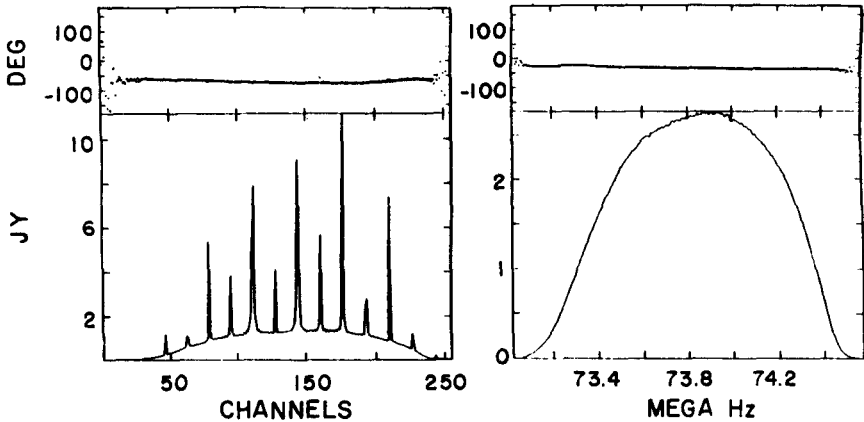shields, of which there are currently only four, will be
needed.

Fig.1:   Cross-power spectra between unshielded
(Fig. 1a, left panel) and shielded (Fig. 1b, right
panel) antenna pairs.

CALIBRATION

Calibration is currently the single biggest challenge facing
the new system. Amplitude calibration can be based on
observations of small diameter sources such as 3C295 (90 Jy at
73.8 MHz). However, we cannot use such observations for phase
calibration of target sources, as phase errors introduced by
the ionosphere change rapidly with time and position on the
sky. On a medium (10 km) baseline, raw phases can drift at
rates of up to 1 degree/second. Fortunately the change is
smooth and can easily be followed by existing phase
calibration algorithms. However, the phase solution derived
from a calibrator observation made at a different time and
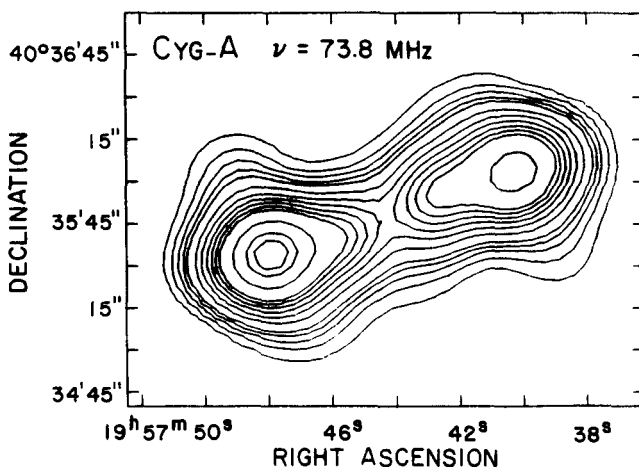
towards a different location in the sky cannot be applied to the source of interest.

This situation forces us to rely upon phase self-calibration techniques based on models of our sources. Fortunately, simple models are usually sufficient for our purposes. For example, we find that VLA 90 or 20 cm maps made in the "C" and "D" configurations provide adequate models for our 73.8 MHz observations made in the "A" configuration. We anticipate a more direct method of phase calibration in which 90 cm data is obtained simultaneously with the 73.8 MHz data. The 90 cm phase solutions could then be scaled by wavelength and directly applied to properly phase our 73.8 MHz data. Test observations in this so-called "4P" mode of the VLA operation are currently underway.

OBSERVATIONS

We have made "A" array VLA observations (maximum resolution ~20" at 73.8 MHz) of four strong radio sources to test the new system. Two of these, 3C144 (the Crab nebula) and 3C461 (Cassiopeia-A) are Galactic Supernova remnants. The other two, 3C405 (Cygnus-A) and 3C274 (Virgo-A), are powerful extragalactic radio galaxies. Maps of three of these sources follow, along with brief descriptions of each. In addition, further test observations of weaker sources are currently underway.

Cygnus-A (right) is the brightest extragalactic radio source in the sky. It has a flux density of 18,000 Jy at 73.8 MHz. Our 73.8 MHz map was made with a synthesized beam of 27"x25" FWHP. It shows evidence of the steep spectrum bridge of radio emission linking the prominent radio lobes. Our observations are consistent with evidence for this emission seen on low frequency maps made at 330 MHz (VLA), 151 MHz (MERLIN), and at 85 MHZ (Cambridge).

Cas-A is a shell-type SNR. Our 73.8 MHz map (right) was made with a synthesized beam of 33"x22" (FWHP). Correspondence between this map and those made at higher frequencies is good, yet several features show clear differences. These differences may be important, as they relate to changes in spectral index across SNRs which in turn relate to the energy distribution and evolution of the relativistic electrons powering SNRs. In the past, low frequency radio observations have had too poor angular resolution to make similar comparisons with higher frequency maps.

CAS-A ν = 73.8 MHz

The Crab nebula is a plerionic (filled-center) SNR. Our 73.8 MHz map (below) is made with a synthesized beam of 26"x23". Greater sensitivity and better coverage will be required to detect the steep-spectrum pulsar buried within the SNR.

Virgo-A (M87) is a nearby (18 Mpc) radio Galaxy with a compact central component, a narrow jet, steeper spectrum radio lobes, and an extended halo. Our 73.8 MHz map (not shown here) reveals radio emission associated with the lobes, and elongated in a direction parallel to the jet. We expect future observations in more compact VLA configurations will detect emission associated with the steep spectrum halo.

CRAB NEBULA ν = 73.8 MHz
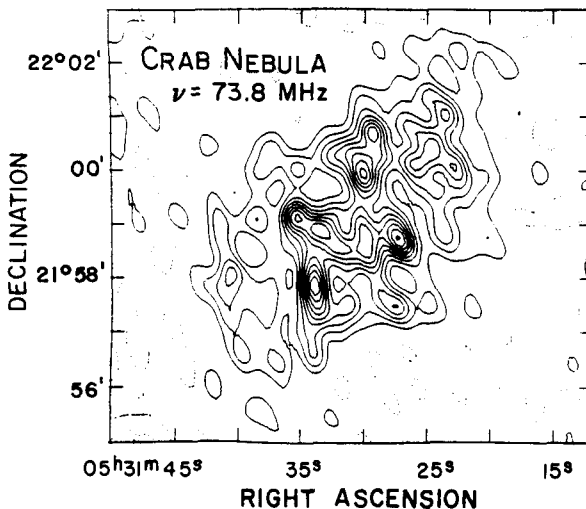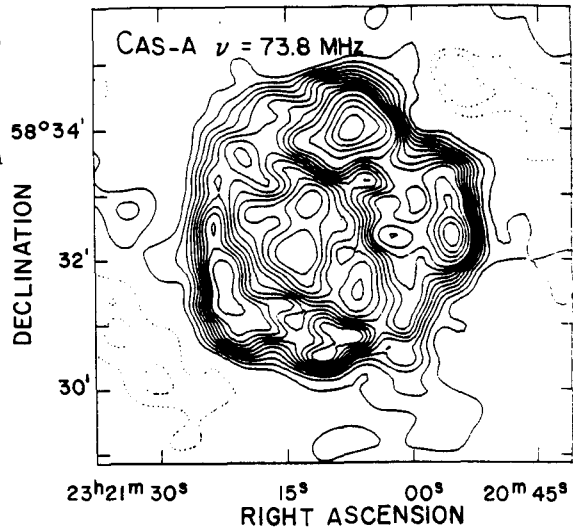
WIDE FIELD MAPPING OF 5C12

J.E. OKOPI and L.B. BÅÅTH

Onsala Space Observatory, S-439 00 Onsala, Sweden.

INTRODUCTION

The existing method of producing radio maps from interferometric data set
is based on the assumption that there is a two dimensional fourier transform
relationship between the sky brightness and the measured visibility. In
mapping of a very wide field, this basic assumption breaks down due to various
practical problems, e.g. bandwidth smearing. We present a wide-field mapping
technique which is aimed at resolving some of these problems. This technique
has been successfully applied to our MERLIN observations of the 5C12 region
covering an area of 1800"x1800".

THE OBSERVATION AND MAPPING PROCEDURE

The observation was made with the MERLIN array in 1983 at 408 MHz, using
the multichannel mode (20 channels). The MERLIN data were read into
the astronomical image processing system (AIPS). The maps presented in
this paper have been produced on the Convex C1 computer with AIPS. The
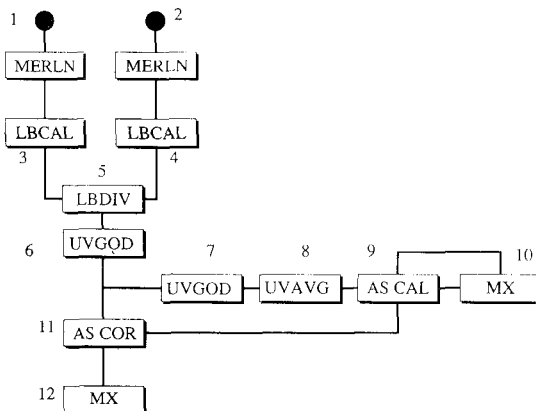mapping procedure is summarized below.

Fig. 1.   5C12 mapping sequence.

(1) Calibration source (0202+14R).
(2) MERLIN data.
(3) Calibrate (0202+14R) and (4) Calibrate MERLIN data.
(5) Correct bandpass with calibration source 0202+14R.
(6) Remove four noisy channels (1,2,19,20).
(7) Rotate to the reference source (5C12.216) and average in frequency.
(8) Average in time to reduce the number of visibility points.
(9) Do phase solution.
(10) Divide the whole field to 16 subfields, deconvolve with CLEAN and map.
(11) Apply solution to original data set.
(12) Map again. Repeat until final CLEAN maps are produced.

RESULT AND DISCUSSION

The resulting maps have a dynamic range of 1000:1. The position of the sources identified has good agreement with those in the Cambridge catalog (see TABLE I below).

TABLE I   Source positions (Cambridge) and Flux density

| Source | Positions | | Flux |
	$\alpha(1950.0)$	$\delta(1950.0)$	(mJy)
5C12.163	12 58 57.56	35 35 11.8	30
5C12.188	13 00 06.06	35 09 26.2	111
5C12.182	13 59 45.34	35 12 46.8	151
5C12.216	13 01 32.92	35 25 55.2	933
5C12.214	13 01 32.50	35 34 43.0	24
5C12.230	13 02 13.80	35 39 37.0	743
5C12.196	13 00 33.82	36 06 16.2	596
5C12.220	13 01 40.40	35 16 05.0	39
5C12.242	13 02 59.00	35 15 39.0	386
5C12.207	13 01 10.41	34 57 52.0	19
5C12.192	13 00 23.15	35 13 58.0	36
5C12.227	13 02 07.50	34 56 49.0	16
5C12.203	13 00 49.34	35 13 54.7	12
5C12.193	13 00 25.13	35 44 24.9	98
5C12.200	13 00 43.23	35 38 39.7	22
5C12.234	13 02 31.60	35 15 52.0	57

The effect of bandwidth smearing was resolved in stage 5 of our mapping procedure. However, the problem due to sky curvature still remains unsolved and it is reflected as elongated structures in some of the sources (e.g., 5C12.242 and 5C12.230) located far away from the reference source (5C12.216). The solution of this problem would require the development of a three-dimensional CLEAN algorithm. However, the computational effort and cost for such work would be very high.
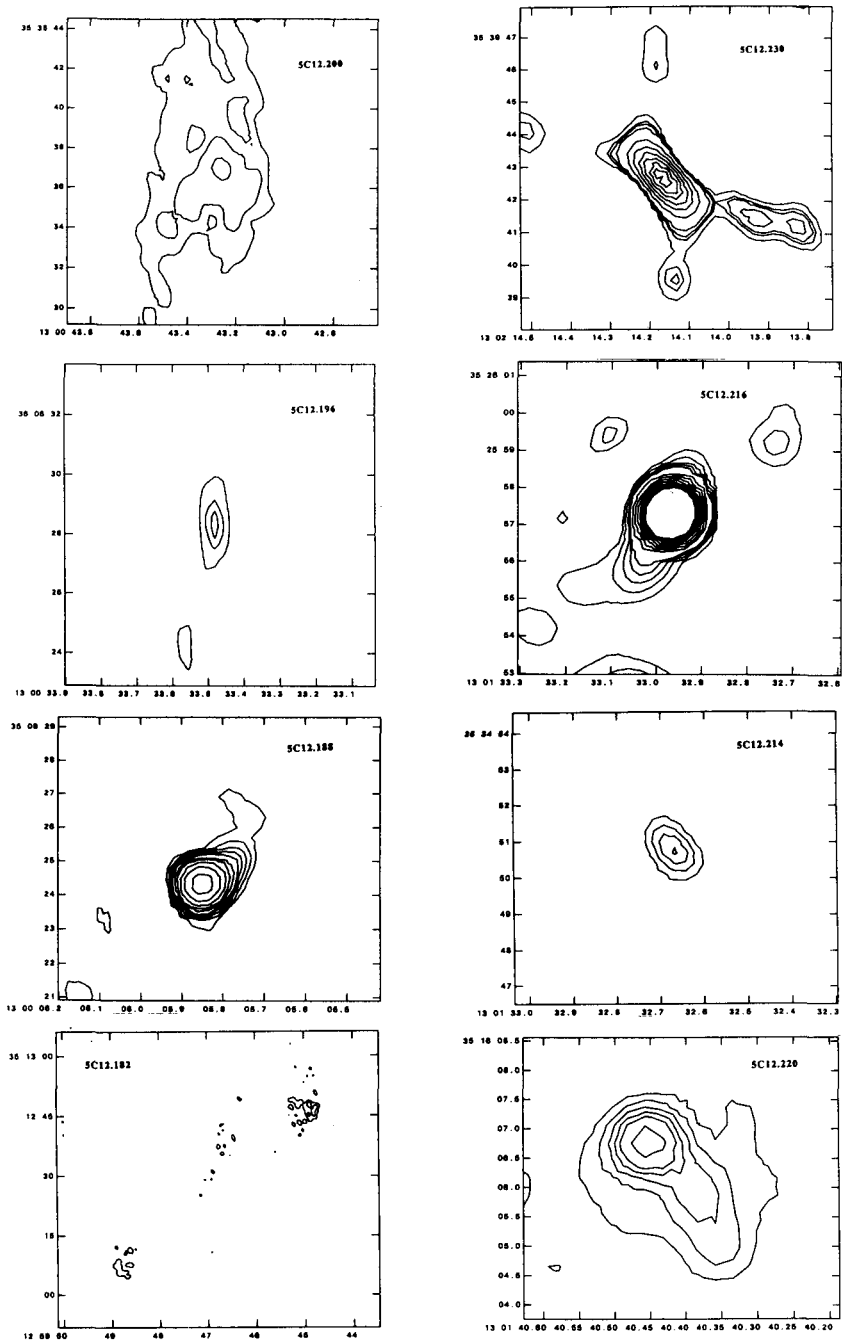
Fig. 2.   5C12 maps (X-axis is right ascension, Y-axis is declination)